Supplementary Materials for

Machine learning-based prediction of clinical pain states using multimodal neuroimaging and autonomic biomarkers

Authors: Jeungchan Lee[1], Ishtiaq Mawla[1], Jieun Kim, Marco L. Loggia, Ana Ortiz, Changjin Jung, Suk-Tak Chan, Jessica Gerber, Vincent J Schmithorst, Robert R. Edwards, Ajay D. Wasan, Chantal Berna, Jian Kong, Ted J. Kaptchuk, Randy L. Gollub, Bruce R. Rosen, Vitaly Napadow[2]

[1]JL and IM contributed equally to this work.

[2]Corresponding author: Vitaly Napadow
Address: Martinos Center for Biomedical Imaging, Building 149, suite 2301, Charlestown, MA 02129. Phone: +1 617-724-3402. Fax: +1-617-726-7422. Email: vitaly@mgh.harvard.edu

This PDF includes:

Page #

Supplemental methods and results
Section S1. Functional localization of primary somatosensory (S1) back region 2
Section S2. Head motion and its contribution towards classification and regression 4

Supplementary figures
Fig. S1. Flowchart outlining data collected, excluded, and analyzed 6

Supplementary tables
Table S1. Brain rCBF features (significant paired-SVM weights) significantly contributing to within-patient classification of lower- versus higher-clinical pain intensity states 7
Table S2. Brain $S1_{CONN}$ features (significant paired-SVM weights) significantly contributing to within-patient classification of lower- versus higher-clinical pain intensity states 9

References 13

Section S1. Functional localization of primary somatosensory (S1) back region

For functional localization seed definition, event-related BOLD fMRI data were preprocessed using tools available with SPM (Statistical Parametric Mapping, https://www.fil.ion.ucl.ac.uk/spm), FSL (FMRIB's Software Library, https://fsl.fmrib.ox.ac.uk/fsl/fslwiki/), AFNI (Analysis of Functional NeuroImages, https://afni.nimh.nih.gov), and FreeSurfer (https://surfer.nmr.mgh.harvard.edu).

The nociceptive primary somatosensory cortex (S1) representation for the low back was localized for functional seed connectivity analysis using the same BOLD EPI pulse sequence as noted for resting connectivity BOLD fMRI in main text. In two fMRI scan runs, chronic low back pain patients (N = 79) and healthy controls (N = 34) were stimulated using painful and non-painful electrical stimuli delivered to the right lower back with electrodes placed over the erector spinae muscles. Stimulation intensity (electrical current, mA) was individually calibrated and applied over 13 painful (target: 40 out of 100, 0 = 'no pain', 100 = 'most intense pain imaginable', current intensity = 3.5 ± 2.9 mA) and 13 non-painful (target: 7 out of 10, 0 = 'no sensation', 10 = 'on the verge of pain'; current intensity = 1.5 ± 1.4 mA) stimuli, randomized in order over the fMRI scan run. Each constant-current stimulation (GRASS S88X, Astro-Med, Inc., RI, USA) was applied for 2 seconds in duration and at 25 Hz, with jittered inter-stimulus interval ranging from 6 to 12 seconds. After each fMRI scan run, perception intensity was verbally rated for painful (48.4 ± 19.4/100) and non-painful (3.8 ± 2.0/10) stimuli.

Collected fMRI data were preprocessed for statistical analysis: physiological artifact correction (3dretroicor, AFNI) [1], motion correction (mcflirt, FSL), susceptibility-induced distortion correction (topup, FSL), skull stripping (bet, FSL), and functional-to-functional alignment (flirt, FSL). After spatial smoothing (FWHM = 5 mm), and temporal filtering (high-pass cutoff frequency = 0.024 Hz), general linear modeling (GLM, FEAT, FSL) was performed

to estimate difference in brain responses to painful and non-painful electrical stimulation. Resultant outputs such as parameter estimates and their variances were fed into a second level analysis for each subject (fixed effects model, FEAT, FSL). These results were then co-registered to a common (MNI, Montreal Neurological Institute) space (bbregister, FreeSurfer) [2] and passed up to a mixed effects group analysis (FLAME1+2, FEAT, FSL). The averaged difference in S1 responses to painful versus non-painful low back stimulation was similar across patients and healthy controls (peak X/Y/Z location in MNI space = -18/-38/72 mm) and localized the S1 somatotopic representation of the low back to create a bilateral $S1_{back}$ seed for defining the whole brain $S1_{back}$ connectivity parameter for our machine learning analysis.

Section S2. Head motion and its contribution towards classification and regression

Head motion can significantly confound pain neuroimaging parameters. Hence, motion during resting BOLD fMRI and PCASL runs, collected before and after physical maneuvers, was estimated as a mean of relative (i.e., TR-to-TR) translation [3]. We also evaluated the number of censored time-points (fsl_motion_outliers) identified in resting BOLD fMRI runs.

The number of censored time-points from resting-state BOLD fMRI data did not significantly differ between pre- and post-maneuvers (pre-maneuver: 6.72±3.28 mm, post-maneuver: 6.32±2.98 mm, paired *t*-test $P = 0.46$). However, relative head motion was significantly different between pre- and post-maneuver BOLD fMRI scans (pre-maneuver: 0.036±0.017 mm, post-maneuver: 0.044±0.023 mm, $P = 0.008$). In ASL runs, there were no significant differences in head motion estimates between pre- and post-maneuver (pre-maneuver: 0.064±0.031 mm, post-maneuver: 0.068±0.036 mm, $P = 0.33$).

Given these results, while we performed several different motion correction procedures and head motion-related residuals were regressed out during preprocessing steps, head motion-related bias may have still influenced our resting BOLD fMRI metrics (i.e. $S1_{CONN}$) for classification between lower and higher clinical pain intensity states. Thus, additional analyses were performed, whereby we included resting state BOLD fMRI head motion parameters as a separate parameter for classification.

Specifically, we included resting state BOLD fMRI head motion (i.e. relative TR-to-TR translation) as a separate parameter for classification (i.e., in addition to rCBF, $S1_{CONN}$, and HF_{HRV}) to investigate potential contribution of head motion artifact to multivariate within-subject SVM classification of clinical pain intensity states and between-subjects SVR with clinical pain ratings. We found that for SVM classification, relative head motion showed no significant contribution ($P = 0.31$) while other parameters remained significant contributors (rCBF: $P <$

0.001, $S1_{CONN}$: $P < 0.001$, HF_{HRV}: $P = 0.01$; Accuracy = 92.45%, AUC = 0.97, TP/FP/FN/TN = 49/4/4/49, which are identical values to our 3-parameter SVM classification model without the head motion parameter). Head motion also demonstrated no significant contribution to multimodal between-subject SVR prediction ($P = 0.30$), where the correlation coefficients between predicted and true clinical pain intensity ratings were not very different when head motion was included as an extra parameter (training dataset: Pearson's $r = 0.51$, testing dataset: $r = 0.628$), compared to correlation coefficients without this parameter (training dataset: $r = 0.52$, testing dataset: $r = 0.635$).

These results demonstrated that while we observed a significant difference in relative head motion between pre-maneuver and post-maneuver BOLD fMRI scan runs, head motion was not an informative/influential factor to classification and prediction. In other words, any residual impact due to head motion was well controlled by our preprocessing steps and did not confound our SVM and SVR results. Furthermore, this result also demonstrated the importance of selecting clear physiological parameters for which confound variables such as head motion can be controlled, thereby aiding multivariate machine learning algorithms for prediction of pain states and ratings.

Supplementary Figures

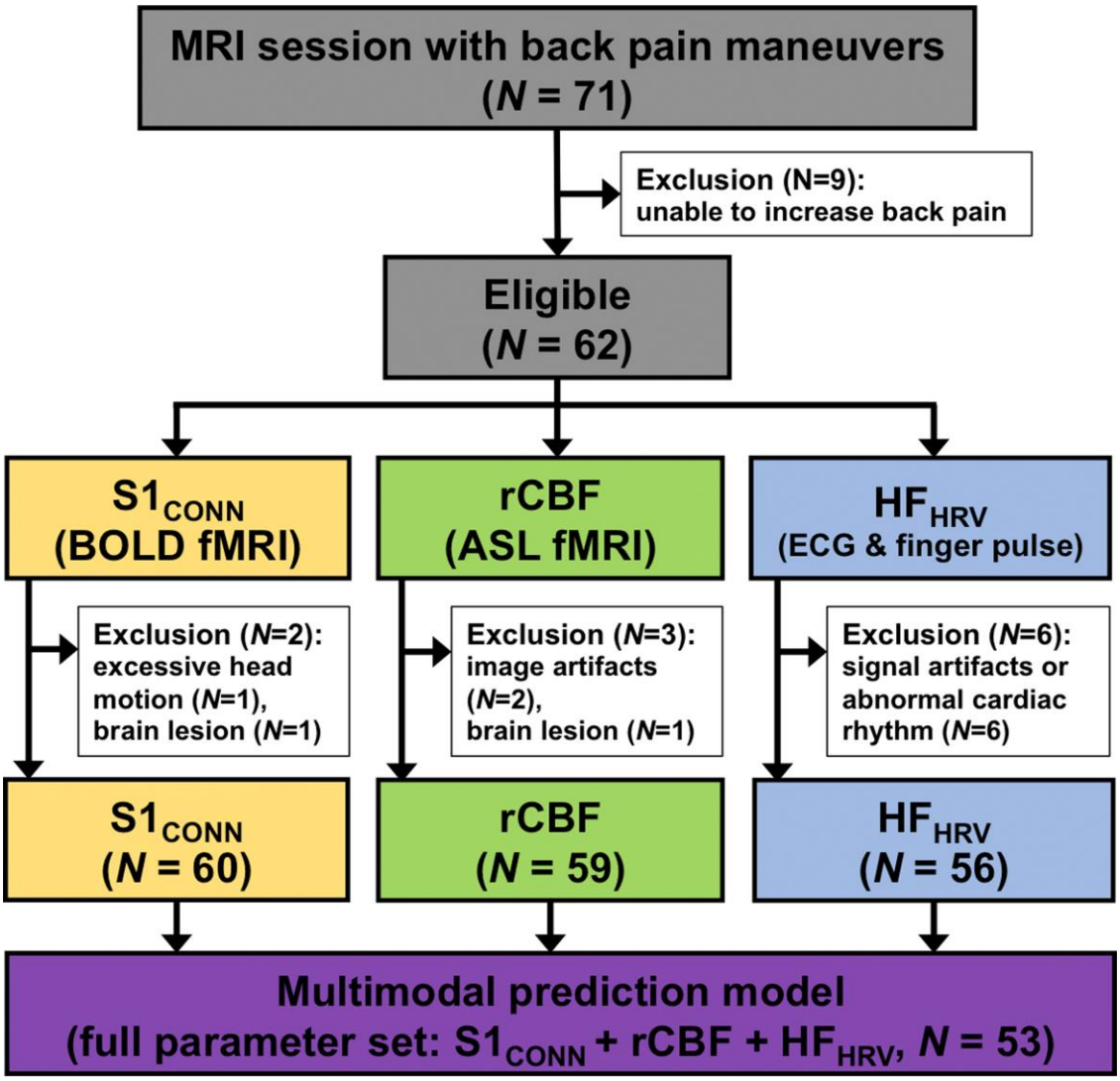

Fig. S1. Flowchart outlining data collected, excluded, and analyzed.

rCBF: regional cerebral blood flow, $S1_{CONN}$: S1-connectivity, HF_{HRV}: high frequency power of heart rate variability, BOLD: Blood Oxygenation-Level Dependent, ASL: Arterial Spin Labeling.

Supplementary Tables

Table S1. Brain rCBF features (paired-SVM weights) significantly contributing to within-patient classification of lower- versus higher-clinical pain intensity states.

Regions	Side	Voxels	Location (MNI, mm) X	Y	Z	Z-score
Positive SVM weights						
posterior cingulate cortex	M	620	0	-58	10	3.37
angular gyrus	L	20	-28	-86	36	3.01
dorsolateral prefrontal cortex	L	54	-18	42	42	2.87
cuneus	L	33	-6	-92	34	2.85
cuneus	R	35	20	-88	40	2.84
supramarginal gyrus	L	77	-58	-60	28	2.82
angular gyrus	L	40	-40	-66	52	2.65
supplementary motor area	M	208	0	-12	56	2.61
dorsolateral prefrontal cortex	L	108	-40	24	40	2.51
middle temporal gyrus	L	12	-62	-8	-28	2.51
angular gyrus	R	23	56	-66	26	2.47
thalamus (ventral posterolateral)	R	22	18	-20	4	2.38
middle frontal gyrus	L	23	-34	60	0	2.37
lingual gyrus	R	30	10	-44	-2	2.36
angular gyrus	R	29	62	-54	30	2.35
middle orbital gyrus	R	54	26	64	-6	2.28

Negative SVM weights

primary somatosensory/motor cortex	L	1108	-50	-12	50	-3.62
superior temporal gyrus	L	558	-38	-38	16	-3.59
primary somatosensory/motor cortex	L	194	-6	-22	76	-3.08
superior parietal lobule	R	199	24	-52	54	-3.05
primary somatosensory cortex	R	430	64	-10	34	-2.81
lingual gyrus	L	61	-12	-74	-4	-2.78
primary motor cortex	R	13	2	-24	74	-2.75
precuneus	R	91	28	-70	6	-2.73
parahippocampal gyrus	L	328	-42	-22	-30	-2.72
superior frontal gyrus (frontal pole)	R	12	8	72	-2	-2.67
superior temporal gyrus	R	35	64	-30	10	-2.66
medial prefrontal cortex	L	40	-10	68	-10	-2.64
occipital gyrus	R	13	16	-72	-10	-2.54
anterior cingulate cortex (subgenu)	L	13	-6	18	-12	-2.53
amygdala	L	13	-20	2	-26	-2.48
superior temporal gyrus	R	396	42	-4	-12	-2.46
primary somatosensory cortex	R	15	4	-40	74	-2.43
cuneus	L	56	-8	-82	20	-2.40

Clusters greater than 10 voxels were reported. rCBF: regional cerebral blood flow, R/M/L: right/medial/left hemisphere.

Table S2. Brain $S1_{CONN}$ features (significant paired-SVM weights) significantly contributing to within-patient classification of lower- versus higher-clinical pain intensity states.

Regions	Side	Voxels	Location (MNI, mm) X	Y	Z	Z-score
Positive SVM weights						
angular gyrus	L	426	-32	-86	22	4.08
inferior frontal gyrus (opercular)	R	100	44	24	12	4.05
cerebellum	L	84	-26	-56	-22	4.05
primary motor cortex	R	282	48	6	42	4.03
anterior middle cingulate cortex	R	94	10	12	32	3.97
superior parietal lobule	R	144	24	-48	76	3.89
cerebellum	L	121	-16	-68	-22	3.84
inferior parietal lobule / supramarginal gyrus	L	631	-56	-56	46	3.76
middle frontal gyrus	R	150	32	26	58	3.74
inferior temporal gyrus	R	104	46	-48	-14	3.68
occipital gyrus	L	107	-24	-74	-12	3.64
inferior temporal gyrus	R	124	46	-72	-8	3.53
dorsal posterior cingulate cortex	L	60	-10	-46	38	3.53
pre-supplementary motor area	L	208	-4	32	46	3.46
middle temporal gyrus	R	314	68	-12	-16	3.43
precuneus	R	159	10	-54	30	3.21
cerebellum	L	60	-44	-74	-40	3.17
dorsolateral prefrontal cortex	R	94	44	36	34	3.12

inferior parietal lobule	R	683	42	-60	58	3.09
frontoinsular cortex	L	328	-56	18	4	3.04
primary motor cortex	L	95	-56	-4	8	3.03
cerebellum	L	51	-28	-34	-32	2.98
superior/inferior parietal lobule	L	64	-40	-58	58	2.95
inferior frontal gyrus (opercular)	L	132	-48	10	22	2.91
rostromedial prefrontal cortex	R	60	2	50	30	2.87
lingual/fusiform gyrus	R	125	30	-42	-10	2.81
primary motor cortex	R	122	14	-6	72	2.73
putamen	L	54	-24	10	-2	2.73
cerebellum	L	134	-54	-62	-30	2.63
paracentral lobule	L	112	-4	-12	58	2.56
dorsal posterior cingulate cortex	L	58	-6	-52	24	2.54
inferior temporal gyrus	L	78	-58	-52	-16	2.43
middle temporal gyrus	L	77	-46	42	22	2.43
Negative SVM weights						
thalamus (ventral posterolateral)	L	53	-14	-20	-4	-4.56
primary motor cortex	L	214	-26	-10	50	-4.52
primary somatosensory/motor cortex	R	907	30	-26	74	-3.95
inferior temporal gyrus	L	65	-38	10	-36	-3.87
posterior middle cingulate cortex	M	166	0	-12	48	-3.66
superior/middle temporal gyrus	R	491	70	-36	2	-3.48

cerebellum	L	69	-24	-78	-54	-3.38
inferior temporal gyrus	R	82	44	-10	-30	-3.24
hypothalamus	R	445	2	0	-12	-3.14
primary somatosensory/motor cortex	L	98	-38	-24	48	-3.14
superior frontal gyrus	R	64	26	2	62	-3.05
cerebellum	M	86	0	-48	-44	-3.04
medial prefrontal cortex	L	61	-2	68	8	-3.04
primary somatosensory/motor cortex	L	159	-46	-16	60	-3.01
medial prefrontal cortex	M	261	0	60	-4	-3.00
superior temporal gyrus	R	73	66	-50	22	-3.00
occipital gyrus	R	152	16	-96	22	-2.96
occipital gyrus	L	104	-10	-104	12	-2.95
primary somatosensory cortex	L	107	-22	-28	60	-2.93
dorsal posterior cingulate cortex	M	80	0	-28	30	-2.91
lingual gyrus	R	53	10	-40	-10	-2.82
occipital gyrus	R	58	34	-84	-20	-2.78
cuneus	R	233	18	-80	38	-2.75
middle frontal gyrus	R	54	40	10	48	-2.69
cerebellum	R	60	12	-42	-58	-2.43
piriform gyrus	R	72	16	4	-18	-2.40
cerebellum	R	72	34	-68	-20	-2.25

Clusters greater than 50 voxels were reported. $S1_{CONN}$: S1-connectivity, R/M/L: right/medial/left hemisphere.

References

[1] Glover GH, Li TQ, Ress D. Image-based method for retrospective correction of physiological motion effects in fMRI: RETROICOR. Magnetic resonance in medicine 2000;44(1):162-167.

[2] Greve DN, Fischl B. Accurate and robust brain image alignment using boundary-based registration. Neuroimage 2009;48(1):63-72.

[3] Van Dijk KR, Sabuncu MR, Buckner RL. The influence of head motion on intrinsic functional connectivity MRI. Neuroimage 2012;59(1):431-438.